Time and magnitude dependent masking effects of vehicle's 2 Hz shock type vibrations on the perception of vehicle's 4.5 Hz longitudinal shock type vibrations for seated human subjects

Nils Bulthaupt* and Frank Gauterin

Institute of Vehicle System Technology,
Karlsruhe Institute of Technology,
Rintheimer Querallee 2,
Gebäude 70.04,
76131, Karlsruhe, Germany
Email: nils.bulthaupt@daimler.com
Email: frank.gauterin@kit.edu
*Corresponding author

Abstract: In the literature there are no known studies regarding temporal masking effects of a vehicle's shock type vibrations. Since shock type vibrations of different directions of movement, magnitudes and frequencies are acting on the human body while driving a vehicle, temporal masking effects may be relevant when evaluating a vehicle's ride comfort. This study investigates temporal post-masking effects of a vehicle's 2 Hz shock type vibrations (masker) on the perception of 4.5 Hz longitudinal shock type vibrations (test signal) for the seated human body. It was found that post-masking exists for the investigated vibrations. The masking effect is highly dependent on the time gap between masker and test signal: with increasing time gap the masking effect decreases. Furthermore the amount of masking increases with increasing masker magnitude. Both findings are consistent with the findings in psychoacoustics. In addition to that the masking effect depends on the masker's direction of movement.

Keywords: vehicle's shock type vibrations; ride comfort; human vibration perception; whole-body vibration; temporal masking effects; forward masking; post-masking; seated human body; heavy duty trucks; ride simulator.

Reference to this paper should be made as follows: Bulthaupt, N. and Gauterin, F. (2019) 'Time and magnitude dependent masking effects of vehicle's 2 Hz shock type vibrations on the perception of vehicle's 4.5 Hz longitudinal shock type vibrations for seated human subjects', *Int. J. Vehicle Noise and Vibration*, Vol. 15, No. 4, pp.256–278.

Biographical notes: Nils Bulthaupt is a Doctoral Researcher at the Institute of Vehicle System Technology at the Karlsruhe Institute of Technology (KIT) in Karlsruhe, Germany. His research project is the objectification of ride comfort for heavy duty trucks. Furthermore he is employed as an automotive engineer for ride simulations at the Daimler AG in Sindelfingen, Germany.

Frank Gauterin is the Managing Director of the Institute of Vehicle System Technology at the Karlsruhe Institute of Technology (KIT) in Karlsruhe, Germany. Furthermore, he is the scientific spokesperson of the KIT Mobility Systems Center and of the local research cluster Profilregion Mobilitaetssysteme Karlsruhe.

1 Introduction

The human perception of vibration depends on various factors, such as vibration frequency, vibration magnitude (e.g., Griffin (1996), Bellmann et al. (2000), Mansfield and Griffin (2000), Baumann et al. (2001), Bellmann et al. (2004), Bellmann and Remmers (2004), Morioka and Griffin (2006), Griffin (2007), Forta et al. (2009), Morioka and Griffin (2010) and Forta et al. (2011)), type of vibration, direction of movement (e.g. Matsumotoa and Griffin (2005), Griffin (2007), Ahn and Griffin (2008), Wyllie and Griffin (2009), Ahn (2010) and Mulder and Abbink (2016)), location of the introduced vibration at the human body (e.g., Griffin (1996), Morioka and Griffin (2005), Forta et al. (2009), Forta et al. (2011), Morioka and Griffin (2015)), posture (e.g., Rakheja and Stiharu (2002), Nawayseh and Griffin (2003), Nawayseh and Griffin (2004), Nawayseh and Griffin (2005a), Nawayseh and Griffin (2005b), Basri and Griffin (2011a), Basri and Griffin (2011b), Qiu and Griffin (2012), Basri and Griffin (2013), Beard and Griffin (2013), Zhou and Griffin (2014) and Beard and Griffin (2016)) and constitution (e.g., Toward and Griffin (2011) and Dewangan et al. (2013)).

One main influencing factor on the human perception of a certain vibration (test vibration) is the existence of another vibration (masker) that occurs simultaneously and weakens or amplifies the perception of the test vibration. The weakening effect is called as masking effect. There are only a few studies dealing with masking effects of vibrations. Morioka and Griffin (2005) investigated the influence of a masking vibration with varying magnitude (Gaussian random vibration centred at 16 Hz or 125 Hz) on the perception threshold of simultaneously excited sinusoidal 16 Hz to 125 Hz vibrations at the middle finger and the whole hand, respectively. In both cases they found that the perception thresholds depend on the masker's magnitude.

In another experiment, Morioka and Griffin (2015) investigated the perception thresholds for 4–31.5 Hz longitudinal sinusoidal backrest vibrations with simultaneous Gaussian random masking vibrations centred at 4 Hz. The masker increased the perception thresholds for each investigated frequency in dependency of the masker's magnitude and the frequency difference between the masker and the test signal. With increasing frequency difference, the influence of the masker on the perception of the test signal decreases.

Ljunggren et al. (2007) investigated the perception of 5–31.5 Hz sinusoidal vertical whole-body vibrations for the seated human body with a simultaneous 8 Hz vertical masker. The masker increases the perception thresholds except for a test vibration of 10 Hz. Furthermore an increased level of discomfort is reported when the test signal frequency gets close to the masker frequency.

Knauer (2010) investigated the perception thresholds for harmonic vibrations, frequency bands and shock type vibrations with a simultaneous masker of different levels and frequency bands. He reported that the masking effect depends on the spectral distance between the test signal frequency and the mid-band frequency of the masker. The masking effect decreases with increasing distance of the frequencies, which is consistent to the investigations of Ljunggren et al. (2007). Furthermore the perception threshold increases with increasing masker level. These results are consistent to the investigations of Morioka and Griffin. However, for whole-body vibrations only the influence of simultaneous masking (the masker occurs at the same time as the test vibration) on the perception of a test vibration has been investigated so far. Temporal masking effects were not taken into account. In psychoacoustics temporal masking effects are subject of many studies (e.g., Zwislocki et al. (1959), Elliott (1962a, 1962b), Zwicker (1965a), Deatherage and Evans (1969), Penner et al. (1974), Moore (1978), Jesteadt et al. (1982); Kidd and Feth (1982), Zwicker (1984), Zwicker and Zwicker (1984), Kollmeier and Gilkey (1990), Plack and Oxenham (1998), Gaskell and Henning (1999) and Oxenham and Plack (2000)). They are separated into three phases of masking: pre-masking (or backward masking) describes the masking effect of a masker which occurs after a test tone and has an influence on the perception of the test tone. Simultaneous masking describes the influence of a masker that occurs at the same time as the test tone. Furthermore post-masking (or forward masking) describes the influence of a masker that appears prior to the test tone. Temporal masking effects in psychoacoustics are highly dependent on

- the time gap between masker and probe tone (the masking effect decreases with increasing time gap (Zwislocki et al., 1959; Elliott, 1962a, 1962b; Zwicker, 1965a; Jesteadt et al., 1982; Zwicker and Zwicker, 1984; Kollmeier and Gilkey, 1990; Gaskell and Henning, 1999; Oxenham and Plack, 2000)
- the duration of the masker (Zwislocki et al., 1959; Elliott, 1962a, 1962b; Zwicker, 1984; Oxenham and Plack, 2000) (the masking effect increases with increasing masker duration (Penner et al., 1974; Kidd and Feth, 1982))
- the magnitude of the masker (the masking effect increases with increasing masker magnitude (Jesteadt et al., 1982; Kidd and Feth, 1982; Oxenham and Plack, 2000))
- the spectral distance between the masker's frequency and the probe tone's frequency (Elliott, 1962a, 1962b; Zwicker, 1965a; Moore, 1978; Jesteadt et al., 1982)
- the duration of the probe tone (Elliott, 1962a, 1962b; Zwicker, 1965a) (the masking effect decreases with increasing probe tone duration (Deatherage and Evans, 1969)).

In the literature there are no known studies regarding temporal masking effects of whole-body vibrations. Since vibrations in different directions of movement, with different magnitudes and frequencies are acting on the seated driver or occupant while driving a vehicle, temporal masking effects may be relevant for vehicle's ride comfort. For heavy duty trucks 1–2 Hz vibrations represent typical cabin movements and 3–6 Hz longitudinal vibrations represent disturbing cabin vibrations on 'good' asphalt roads.

For that reason this study investigates the influence of 2 Hz whole-body shock type vibrations (masker) on the perception of 4.5 Hz longitudinal whole-body shock type vibrations (reference signal) for seated human subjects. On the basis of the findings in psychoacoustics, the effect of the masker is investigated in dependency of time gaps between the masker and the reference signal and also in dependency of the masker's magnitude. In addition to that the masker's direction of movement is also varied.

Major aim of this paper is the determination of weighting factors, which describe the relationship between the perception magnitude of masked and unmasked 4.5 Hz longitudinal shock type vibrations in dependency of the varied parameters. The weighting factors and their dependencies may contribute to a better understanding of the human vibration perception and may therefore be used for vehicle's ride comfort analysis.

2 Method

2.1 Apparatus

The experiments were conducted on the 'Ride Simulator' of the Daimler AG, which is displayed in Figure 1. The Ride Simulator consists of an acceleration controlled movable hexapod platform which is able to perform translational and rotatory movements in all directions of movement. Measured or artificially built acceleration signals can be played by the simulator. The applied coordinate system for referencing the acceleration signals is centred at the front left corner of the driver's seat console. It is shown in Figure 1. The maximum possible displacements of the platform are given as follows: ± 220 mm in x- and y-direction, ± 200 mm in z-direction and ±6° around every axis.

Figure 1 Ride Simulator and applied coordinate system

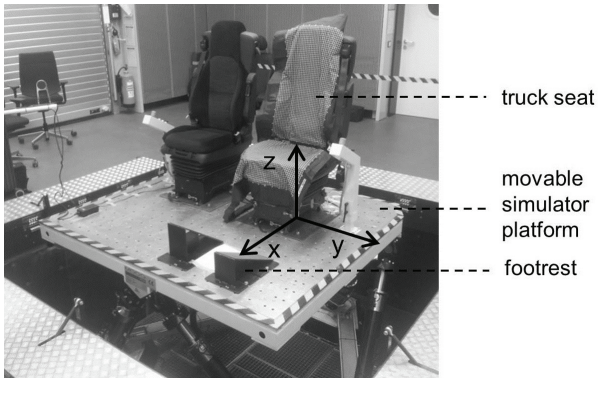

Truck seats (model MSG 115, Grammer AG) and footrests were mounted on the simulator platform to get seating conditions equivalent to a real truck. The subjects were seated on the left seat in driving direction. The seat adjustments were set as follows and remained

constant: The seat pan was inclined by –5° around the y-axis regarding the x-y-plane. The backrest was inclined by –15° around the y-axis regarding y-z-plane. The arm rests were set at the upper position. Furthermore the vertical seat damping was set at the highest level. The mounted footrests allow a gas pedal positioning of the feet. Their settings were adopted from a Mercedes-Benz Actros 4×2 tractor and were set as follows: The left foot rest was inclined by –25° and the right footrest by –35° around the y-axis regarding the x-y-plane.

2.2 Vibration stimuli

The acceleration signals that were applied on the Ride Simulator are referenced on the centre point of the Ride Simulator coordinate system. Each acceleration signal consists of six acceleration components: one acceleration component for each direction of movement. They are named as a_{tx}, a_{ty}, a_{tz}, a_{rx}, a_{ry} and a_{rz}. The index t indicates a translational acceleration. r indicates a rotatory acceleration. x, y and z show the axes of movement.

Acceleration signals that were acquired during test drives at the driver's seat console of a Mercedes-Benz Actros 4×2 truck were used to build the following artificial acceleration signals, which will be used for the Ride Simulator experiments.

2.2.1 Reference signal

The so called 'reference signal' is used as a reference for several variant signals, which will be presented in the following section. The reference signal was built as follows.

In a first step a background acceleration signal was created. Therefore a part of the measured acceleration signals without any significantly perceptible and disturbing vibration phenomena was identified, that gives an impression of a driving truck on a flat road. It has a duration of 3 s and was repeated to get a background signal with a total duration of 12 s. The background signal's RMS-values of each component are $0.18\,\mathrm{m/s^2}$ for a_{tx}, $0.03\,\mathrm{m/s^2}$ for a_{ty}, $0.15\,\mathrm{m/s^2}$ for a_{tz}, $0.3\,\mathrm{rad/s^2}$ for a_{rx}, $0.15\,\mathrm{rad/s^2}$ for a_{ry} and $0.01\,\mathrm{rad/s^2}$ for a_{rz}. In a second step a well perceptible 4.5 Hz longitudinal shock type vibration was cut from the measured truck signals and was then superposed to the background signal at the instant of time $t_R = 9.11$ s. This shock type vibration is from now on called the 'reference event'. The acceleration amplitude of the reference event in the main direction of movement tx is $A_{Ref,tx} = 1.26\,\mathrm{m/s^2}$. The acceleration amplitudes of the other components are $A_{Ref,ty} = 0.08\,\mathrm{m/s^2}$, $A_{Ref,tz} = 0.59\,\mathrm{m/s^2}$, $A_{Ref,rx} = 0.12\,\mathrm{rad/s^2}$, $A_{Ref,ry} = 0.43\,\mathrm{rad/s^2}$ and $A_{Ref,rz} = 0.05\,\mathrm{rad/s^2}$. The whole reference signal (background signal + superposed reference event) is shown in Figure 2(a).

2.2.2 Variant signals

In addition to the presented reference signal, different variant signals were built. The variant signals were created on the basis of the reference signal with an additional shock type vibration (masking event) placed in the same manner as the reference event prior to or simultaneous with the reference event. A shock type vibration of 2 Hz was chosen as a masking event, which represents a cabin movement of a heavy duty truck.

The masking event consists only of one acceleration component in the masking direction of movement $MDoM$, which was varied in all possible six direction of movements tx, ty, tz, rx, ry and rz.

A '+' in front of the direction of movement indicates an initial movement in the positive axis direction and a following movement in negative direction back to the initial state. In

addition to that the amplitude of the masking event $A_{Mask,MDoM}$ was varied in four steps and the time gap between the reference event and the masking event Δt was varied in six steps (Table 1). For calculating Δt the time midpoint of the masking event t_M and the time midpoint of the reference event t_R were used (Figure 2(b)):

$$\Delta t = t_R - t_M. \tag{1}$$

An overview of all parameter variations is given in Table 1. A variant signal was created for each possible parameter combination. In total 144 (6×4×6) variant signals were created. An example is shown in Figure 2(b).

Figure 2 Comparison of: (a) reference signal and (b) variant signal

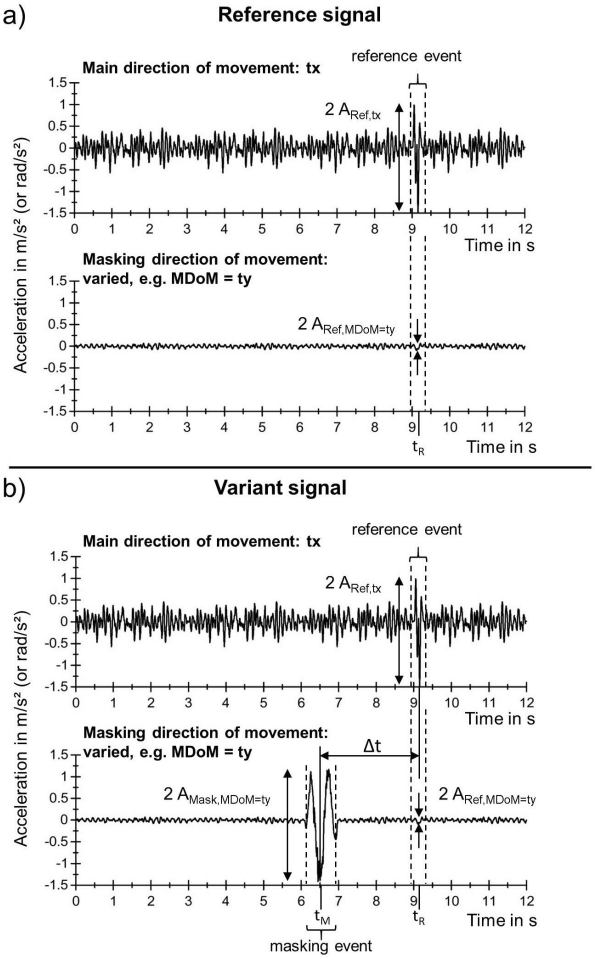

2.3 Subjects

Twelve male human subjects participated at the experiments of this study (mean age: 39.75 (standard deviation SD: 13.07), mean body mass: 82.5 kg (SD: 10.22 kg), mean body height: 181.92 cm (SD: 6.65 cm), mean BMI: 24.94 kg/m^2 (SD: 2.87 kg/m^2)).

Table 1 Parameter variations of the variant signals

Δt *in* s	$A_{Mask,MDoM}$	$MDoM$
0	$0.5A_{Ref,tx}$	$+tx$
0.58	$1A_{Ref,tx}$	$+ty$
1.08	$2A_{Ref,tx}$	$+tz$
1.58	$4A_{Ref,tx}$	$+rx$
2.58		$+ry$
4.58		$+rz$

2.4 Procedure

The variant signals were used for analysing the effect of the masking event on the perception of the reference event by comparing them to the unmasked reference signal.

The investigations were split in six runs of 24 pairwise comparisons. Each run was performed by every subject. In total, each subject evaluated 144 pairwise comparisons.

At the beginning of every run, the reference signal was presented twice to the current human subject (one time with double and one time with a quarter magnitude of the reference event) in order to get familiar with the range of excitation and the used 9-point-evaluation-scale. The lower endpoint '1' represents 'not perceptible'. The upper endpoint '9' represents 'very strong'. Afterwards the pairwise comparisons were played in the following procedure: the reference signal was played first, followed by a 3 s pause and the variant signal. Next the subjective evaluation regarding the perceived strength of the reference event in both signals was done by the current human subject. First the perceived strength of the reference event in the reference signal was evaluated. Then the perceived strength of the reference event in the variant signal was evaluated.

2.5 Analysis

The following measurements were defined for analysing the effect of the masking event on the perception of the reference event and its dependency on time gap, magnitude and the masker's direction of movement.

On the basis of the findings of Fechner (1966), a relative growth of stimuli R_{MDoM} was defined. It describes the ratio between the magnitude of the masking event ($A_{Mask,MDoM}$) in the masking direction of movement ($MDoM$) and the magnitude of the reference event in its main direction of movement (translational movement in x-direction) $A_{Ref,tx}$.

$$R_{MDoM} = \frac{A_{Mask,MDoM}}{A_{Ref,tx}}. \tag{2}$$

The effect of the masking event on the perception of the reference event was determined by defining a masking factor $G_{MDoM}(R_{MDoM}, \Delta t)$.

This masking factor is the median of the human subject dependent masking factors $G_{HS,MDoM}(R_{MDoM}, \Delta t)$. For each human subject $HS \in \{1..12\}$, $G_{HS,MDoM}(R_{MDoM}, \Delta t)$ describes the relation between the subjective rating of the reference event with the influence of the masking event $N_{HS,Mask,MDoM}(R_{MDoM}, \Delta t)$

and the corresponding subjective rating of the reference event without the influence of the masking event $N_{HS,Ref}(R_{MDoM}, \Delta t)$.

$$G_{HS,MDoM}(R_{MDoM}, \Delta t) = \frac{N_{HS,Mask,MDoM}(R_{MDoM}, \Delta t) - 1}{N_{HS,Ref}(R_{MDoM}, \Delta t) - 1} \tag{3}$$

$$\underline{\boldsymbol{G}}_{MDoM}(R_{MDoM}, \Delta t) = \begin{bmatrix} G_{1,MDoM}(R_{MDoM}, \Delta t) \\ G_{2,MDoM}(R_{MDoM}, \Delta t) \\ \vdots \\ G_{11,MDoM}(R_{MDoM}, \Delta t) \\ G_{12,MDoM}(R_{MDoM}, \Delta t) \end{bmatrix} \tag{4}$$

$$G_{MDoM}(R_{MDoM}, \Delta t) = median(\underline{\boldsymbol{G}}_{MDoM}(R_{MDoM}, \Delta t)). \tag{5}$$

Due to the design of the experiments, the reference event in the reference signal is always perceptible. From this follows $N_{HS,Ref}(R_{MDoM}, \Delta t) - 1 > 0$. Values of $G_{HS,MDoM}(R_{MDoM}, \Delta t) < 1$ express a masking effect and values of $G_{HS,MDoM}(R_{MDoM}, \Delta t) > 1$ express an amplifying effect on the perception of the reference event under the influence of the masking event.

3 Results

The masking factors $G_{MDoM}(R_{MDoM}, \Delta t)$ are evaluated separately for every $MDoM$ in dependence of R_{MDoM} and Δt. The results are shown in Figure 3 for translational $MDoM$ and in Figure 4 for rotatory $MDoM$. For comparisons the masking factors of the reference signal (defined with $G_{MDoM}(R_{MDoM} = 0, \Delta t) = 1$) are plotted as fat, black lines in each figure.

For analysing significant differences between $G_{MDoM}(R_{MDoM}, \Delta t) \neq 1$ and $G_{MDoM}(R_{MDoM}, \Delta t) = 1$, a Wilcoxon signed rank test is used. $G_{MDoM}(R_{MDoM}, \Delta t) = 1$ corresponds to an equal evaluation as the reference signal. The level of significance is set with 0.05. In Figure 3 and 4 significant values are highlighted with black filled markers. Non-significant values are shown with white filled markers. The detailed significance values are listed in Table A1 in the appendix.

In both Figures 3 and 4 the 2 Hz masking events show an influence on the perception of the 4.5 Hz reference event for all $MDoM$.

For $+ty$, $+rx$, $+ry$ and $+rz$ the masking event affects the perception of the reference event as follows: with increasing R_{MDoM} and decreasing Δt the masking factor $G_{MDoM}(R_{MDoM}, \Delta t)$ decreases, which describes an increasing masking effect. Furthermore the duration of the masking effect increases with increasing R_{MDoM} (e.g., the curve $G_{+ty}(R_{+ty} = 0.5, \Delta t)$ reaches the value '1' at $\Delta t = 1.58$ s, while $G_{+ty}(R_{+ty} = 4, \Delta t)$ reaches the value '1' at $\Delta t = 4.58$ s). The same trends can be found for $+tz$ with an exception for $G_{+tz}(R_{+tz} = 0.5, \Delta t = 0.58\text{ s})$. All $G_{MDoM}(R_{MDoM}, \Delta t) \neq 1$ are significant for $+ty$, $+tz$, $+rx$, $+ry$, and $+rz$.

In all five masking directions of movement and for all R_{MDoM} simultaneous masking ($\Delta t = 0$ s) is more effective than forward masking ($\Delta t > 0$ s). For $R_{MDoM} = 4$ or $R_{MDoM} = 4\text{rad/m}$ and $\Delta t = 0$ s the masking effect is biggest and the reference event is masked completely by the masking event ($G_{MDoM}(R_{MDoM} = 4, \Delta t = 0\text{ s}) = 0$ and $G_{MDoM}(R_{MDoM} = 4\text{rad/m}, \Delta t = 0\text{ s}) = 0$).

Figure 3 Masking factors $G_{MDoM}(R_{MDoM}, \Delta t)$ for translational 2 Hz masking events with varying time gap Δt, relative growth of stimuli R_{MDoM} and varying masking directions of movement $MDoM$ (black filled markers: significant masking factor values)

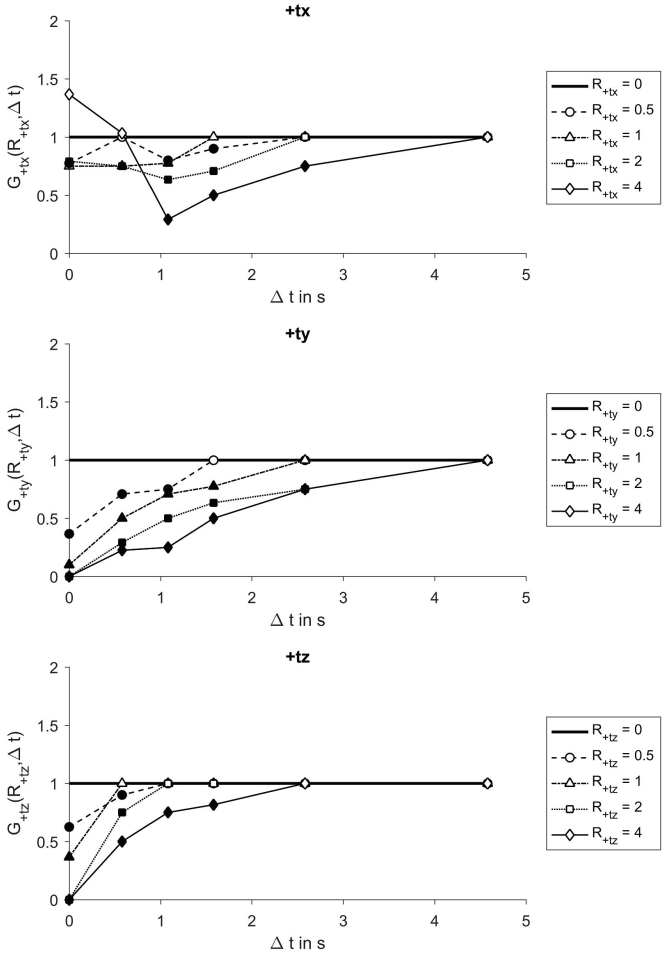

The masking direction of movement $+tx$ (which is also the reference event's main direction of movement) shows a different behaviour than the other masking directions of movement. For $R_{MDoM} = 4$ a non-significant amplifying effect is occurring, which is decreasing with increasing Δt and then turning into a significant masking effect at $\Delta t = 1.08$ s which is also decreasing with increasing Δt. The other R_{MDoM} show only weak masking effects in comparison to the other $MDoM$. The masking effects are also significant except for $G_{+tx}(R_{+tx} = 0.5, \Delta t = 0.58 \text{ s})$.

Figure 4 Masking factors $G_{MDoM}(R_{MDoM}, \Delta t)$ for rotatory 2 Hz masking events with varying time gap Δt, relative growth of stimuli R_{MDoM} and varying masking directions of movement $MDoM$ (black filled markers: significant masking factor values)

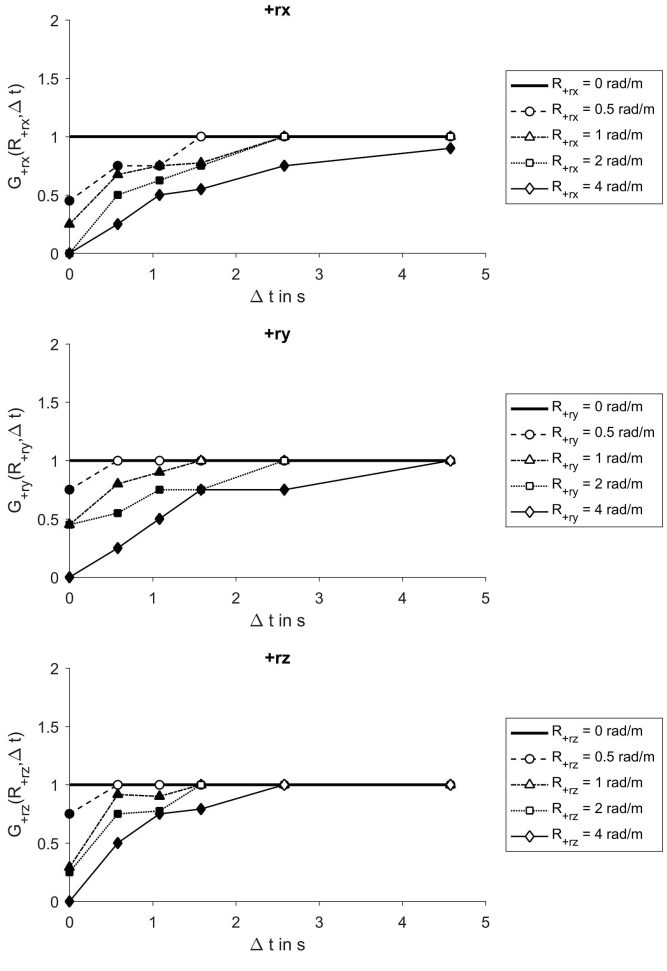

4 Discussion

For a mathematical description of the results the following parametrised exponential approach is proposed to fit the masking factor curves:

$$\hat{G}_{Fit,MDoM}(R_{MDoM}, \Delta t) = [B_{MDoM}(R_{MDoM}) \cdot \Delta t + C_{MDoM}(R_{MDoM})] \cdot \exp[\Delta t \cdot D_{MDoM}(R_{MDoM})] + 1 \quad (6)$$

$$\hat{G}_{MDoM}(...) = \begin{cases} \hat{G}_{Fit,MDoM}(...) & \hat{G}_{Fit,MDoM}(...) \geq 0 \\ 0 & \hat{G}_{Fit,MDoM}(...) < 0. \end{cases} \quad (7)$$

$\hat{G}_{MDoM}$ is the estimated masking factor. B, C and D are $MDoM$ and R_{MDoM} dependent fitting parameters. The fitting parameter B represents the amount of growth for decreasing

Δt. C represents the condition for simultaneous masking and D represents the amount of growth for increasing Δt.

The proposed approach fits the masking factor curves well. The mean correlation coefficient r is 0.96 with a standard deviation of 0.07. The fitting curves and correlation coefficients for $MDoM = +ty$ are shown in Figure 5. The $G_{+ty}(R_{+ty}, \Delta t)$ values are presented in circles. The distributions of the corresponding $\underline{\boldsymbol{G}}_{+ty}(R_{+ty}, \Delta t)$ values are presented as boxplots (circle: median values (=$G_{+ty}(R_{+ty}, \Delta t)$), bold lines: interquartile ranges, x: spikes). All remaining fitting curves and the corresponding r-values are listed in Appendix in Figures A1–A5.

Figure 5 Fitting curves and correlation values r for $G_{+ty}(R_{+ty}, \Delta t)$ with the distributions of $\underline{\boldsymbol{G}}_{+ty}(R_{+ty}, \Delta t)$

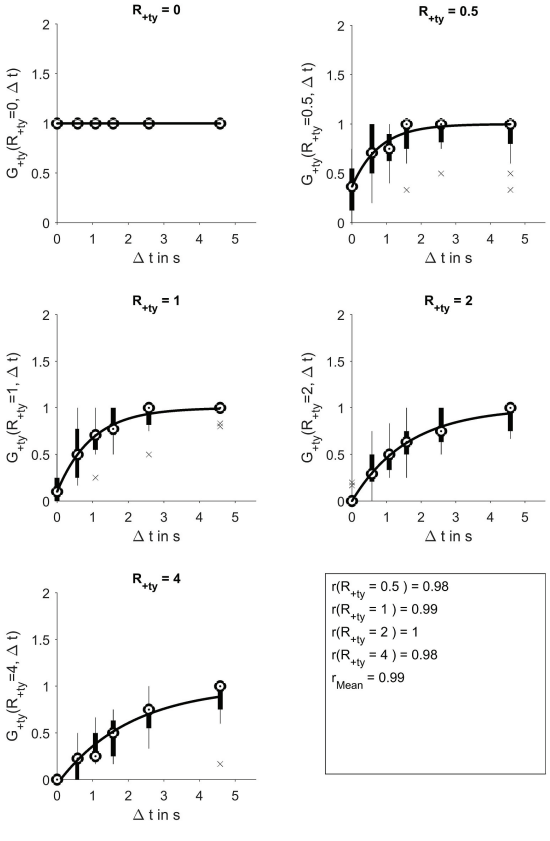

The parameters B, C and D of all fitting curves are shown in Figures 6–8 for all $MDoM$ in dependency of R_{MDoM}. With an interpolation of these parameter values and the application of equations (6) and (7) it is possible to determine masking factors for any R_{MDoM} in the range of the investigated R_{MDoM}.

The parameter curves are highly dependent on the masking direction of movement. Parameter B is only relevant for $+tx$. Parameter C is decreasing in different ways for $+ty$, $+tz$, $+rx$, $+ry$ and $+rz$, representing the increasing simultaneous masking (decreasing $\hat{G}_{Fit,MDoM}$) for increasing R_{MDoM}. $+tx$ shows the amplifying effect for $R_{+tx} = 4$. The

amount of growth of $\hat{G}_{Fit,MDoM}$ for increasing R_{MDoM} is also dependent on $MDoM$: parameter D increases for $+ty$, $+rx$, $+ry$, and $+rz$ in different ways. Exceptions are $+tx$ and $+tz$.

Figure 6 Parameter B in dependency of R_{MDoM}

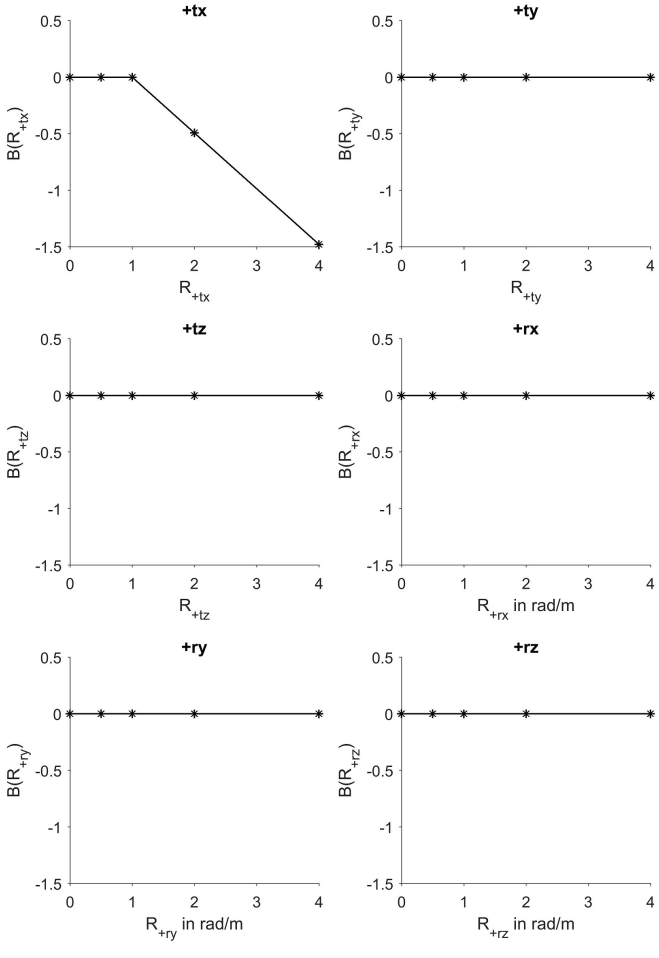

For simultaneous masking the findings are consistent with the findings of Morioka and Griffin (2015), who found an increasing masking effect with increasing masker magnitude for 4–31.5 Hz fore-and-aft sinusoidal backrest vibrations with a simultaneous 4 Hz masker. Since there are no studies regarding temporal masking effects of shock type vibrations, the results may be compared to the findings in psychoacoustics. The findings regarding forward masking in psychoacoustics are consistent to the findings of this study. A decreasing masking

effect with increasing time gap is reported in Elliott (1962a), Zwicker (1965a), Zwicker (1965b), Jesteadt et al. (1982), Zwicker and Zwicker (1984), Zwicker (1984), Gaskell and Henning (1999) and Oxenham (2001). The same influence was found in this study for the investigated shock type vibrations. Also increasing forward masking with increasing masker magnitude is found in psychoacoustics (Jesteadt et al., 1982; Kidd and Feth, 1982; Plack and Oxenham, 1998; Oxenham and Plack, 2000) indicating that equivalent neural effects are responsible for masking effects in psychoacoustics and the reported masking effects in this study. In addition to the consistent influencing factors between this study and psychoacoustics, a dependency of the masking effect on the masker's direction of movement was found in this study.

Figure 7 Parameter C in dependency of R_{MDoM}

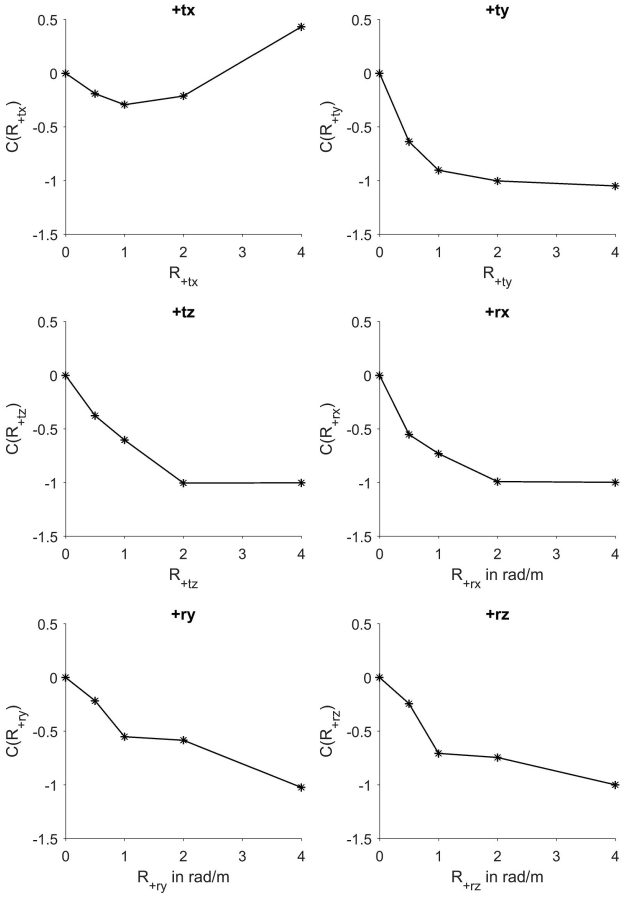

Figure 8 Parameter D in dependency of R_{MDoM}

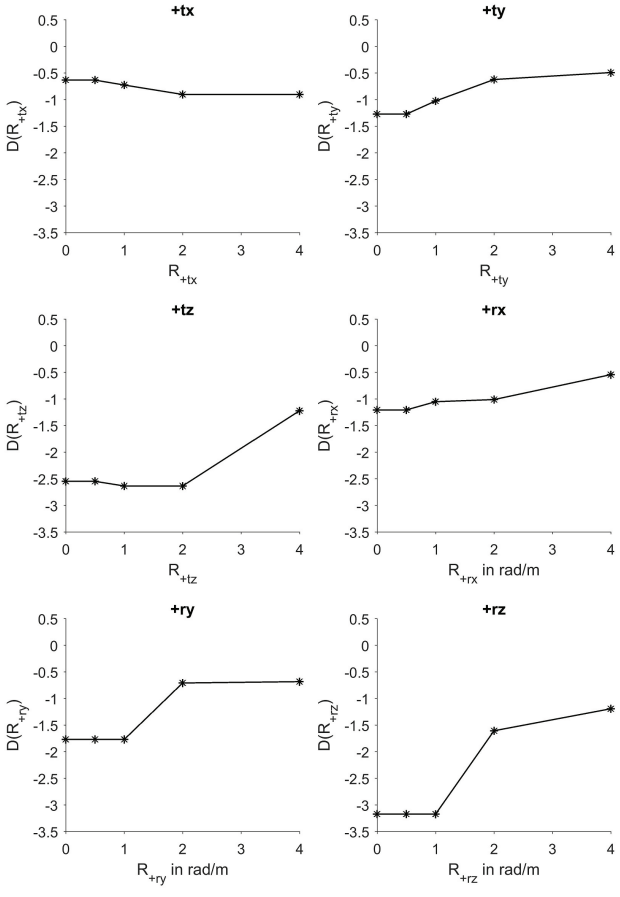

5 Conclusion

The temporal masking behaviour of a vehicle's 2 Hz shock type vibrations (masker) on the perception of the vehicle's 4.5 Hz longitudinal shock type vibrations (test signal) was investigated for the seated human body. The time gap between masker and test signal, the masker's magnitude and also the masker's direction of movement were varied. The amount of masking was expressed via masking factors, which describe the ratio between the perception magnitude of the masked 4.5 Hz longitudinal shock type vibration and the unmasked 4.5 Hz longitudinal shock type vibration.

It was found that post-masking exists for the investigated shock type vibrations. The masking effect is highly dependent on the time gap between masker and test signal: with increasing time gap the masking effect decreases. Furthermore the amount of masking depends on the masker's magnitude: with increasing masker magnitude the masking effect increases. This is consistent with the findings in psychoacoustics. Also the duration of the

masking effect increases with increasing masker magnitude. Furthermore it was found that the amount of masking depends on the direction of movement of the masker.

For determining the masking effect of random low frequency masker magnitudes within the investigated magnitude range, a mathematical exponential approach was proposed to fit the time gap, masker's direction of movement and masker's magnitude dependent masking factor curves. With the well-fitting proposed approach it is possible to calculate the influence of low frequency 2 Hz shock type vibrations on the perception of 4.5 Hz longitudinal shock type vibrations.

The findings may contribute to a better understanding of human vibration perception and may therefore be relevant for a vehicle's ride comfort. The masking effects of low frequency cab or car body movements near to 2 Hz may be used for wheel suspension or cab suspension tunings to cover or weaken perceptible vibrations in the frequency range near to 4.5 Hz. Furthermore the results may be used for an increasing quality of ride comfort prediction models.

Acknowledgements

The study was done during the corresponding author's doctoral researches at the Karlsruhe Institute of Technology (KIT) with kind support of the Daimler AG, who provided all resources and the access to the Ride Simulator. As representatives we would like to thank Mr. Denis Heddergott, Mr. Dr. Manfred Rohr and Mr. Prof. Ludger Dragon for their support.

References

Ahn, S.J. (2010) 'Discomfort of the vertical whole-body shock-type vibration in the frequency range of 0.5 to 16 hz', *International Journal of Automotive Technology*, Vol. 11, No. 6, pp.909–916.

Ahn, S-J. and Griffin, M.J. (2008) 'Effects of frequency, magnitude, damping, and direction on the discomfort of vertical whole-body mechanical shocks', *Journal of Sound and Vibration*, Vol. 311, pp.485–497.

Basri, B. and Griffin, M.J. (2011a) 'The vibration of inclined backrests: perception and discomfort of vibration applied normal to the back in the x-axis of the body', *Journal of Sound and Vibration*, Vol. 330, Nos. 18–19, pp.4646–4659.

Basri, B. and Griffin, M.J. (2011b) 'The vibration of inclined backrests: perception and discomfort of vibration applied parallel to the back in the z-axis of the body', *Ergonomics*, Vol. 54, No. 12, pp.1214–1227.

Basri, B. and Griffin, M.J. (2013) 'Predicting discomfort from whole-body vertical vibration when sitting with an inclined backrest', *Applied Ergonomics*, Vol. 44, No. 3, pp.423–434.

Baumann, I., Bellmann, M.A., Mellert, V. and Weber, R. (2001) 'Wahrnehmungs-und Unterschiedsschwellen von Vibrationen auf einem Kraftfahrzeugsitz', *Fortschritte der Akustik – DAGA 2001*.

Beard, G.F. and Griffin, M.J. (2013) 'Discomfort during lateral acceleration: Influence of seat cushion and backrest', *Applied Ergonomics*, Vol. 44, No. 4, pp.588–594.

Beard, G.F. and Griffin, M.J. (2016) 'Discomfort of seated persons exposed to low frequency lateral and roll oscillation: Effect of backrest height', *Applied Ergonomics*, Vol. 54, pp.51–61.

Bellmann, M.A. and Remmers, H. (2004) 'Evaluation of vibration perception in passenger cabin', *Fortschritte der Akustik – DAGA 2004*.

Bellmann, M.A., Mellert, V., Reckhardt, C. and Remmers, H. (2000) 'Experimente zur Wahrnehmung von Vibrationen', *Fortschritte der Akustik – DAGA 2000*.

Bellmann, M.A., Remmers, H. and Mellert, V. (2004) 'Grundlegende Experimente zur Wahrnehmung von vertikalen Ganzkörpervibrationen – basic experiments on the perception of vertical whole-body vibrations', *VDI Bericht*.

Deatherage, B. and Evans, T. (1969) 'Binaural masking: Backward, forward, and simultaneous effects', *The Journal of the Acoustical Society of America*, Vol. 46, No. 2, pp.362–371.

Dewangan, K.N., Shahmir, A., Rakheja, S. and Marcotte, P. (2013) 'Seated body apparent mass response to vertical whole body vibration: gender and anthropometric effects', *International Journal of Industrial Ergonomics*, Vol. 43, No. 4, pp.375–391.

Elliott, L. (1962a) 'Backward and forward masking of probe tones of different frequencies', *The Journal of the Acoustical Society of America*, Vol. 34, No. 8, pp.1116–1117.

Elliott, L. (1962b) 'Backward masking: Monotic and dichotic conditions', *The Journal of the Acoustical Society of America*, Vol. 4, No. 8, pp.1108–1115.

Fechner, G.T. (1966) *Elements of Psychophysics*, Holt, Rinehart and Winston, New York. original from 1860.

Forta, N.G., Griffin, M.J. and Morioka, M. (2011) 'Difference thresholds for vibration of the foot: Dependence on frequency and magnitude of vibration', *Journal of Sound and Vibration*, Vol. 330, pp.805–815.

Forta, N.G., Morioka, M. and Griffin, M.J. (2009) 'Difference thresholds for the perception of whole-body vertical vibration: dependence on the frequency and magnitude of vibration', *Ergonomics*, Vol. 52, No. 10, pp.1305–1310.

Gaskell, H. and Henning, G. (1999) 'Forward and backward masking with brief impulsive stimuli', *Hearing Research*, Vol. 129, pp.92–100.

Griffin, M.J. (1996) *Handbook of Human Vibration*, Elsevier Academic Press, London.

Griffin, M.J. (2007) 'Discomfort from feeling vehicle vibration', *Vehicle System Dynamics: International Journal of Vehicle Mechanics and Mobility*, Vol. 45, Nos. 7–8, pp.679–698.

Jesteadt, W., Bacon, S. and Lehman, J. (1982) 'Forward masking as a function of frequency, masker level, and signal delay', *The Journal of the Acoustical Society of America*, Vol. 71, No. 4, pp.950–962.

Kidd, G. and Feth, L. (1982) 'Effects of masker duration in pure-tone forward masking', *The Journal of the Acoustical Society of America*, Vol. 72, No. 5, pp.1384–1386.

Knauer, P. (2010) *Objektivierung des Schwingungskomforts bei instationärer Fahrbahnanregung*, PhD thesis, Technische Universität München, Fakultät für Maschinenwesen.

Kollmeier, B. and Gilkey, R. (1990) 'Binaural forward and backward masking: evidence for sluggishness in binaural detection', *The Journal of the Acoustical Society of America*, Vol. 87, No. 4, pp.1709–1719.

Ljunggren, F., Wang, J. and Ågren, A. (2007) 'Human vibration perception from single- and dual-frequency components', *Journal of Sound and Vibration*, Vol. 300, pp.13–24.

Mansfield, N.J. and Griffin, M.J. (2000) 'Difference thresholds for automobile seat vibration', *Applied Ergonomics*, Vol. 31, No. 3, pp.255–261.

Matsumotoa, Y. and Griffin, M.J. (2005) 'Nonlinear subjective and biodynamic responses to continuous and transient whole-body vibration in the vertical direction', *Journal of Sound and Vibration*, Vol. 287, pp.919–937.

Moore, B. (1978) 'Psychophysical tuning curves measured in simultaneous and forward masking', *The Journal of the Acoustical Society of America*, Vol. 63, No. 2, pp.524–532.

Morioka, M. and Griffin, M.J. (2005) 'Independent responses of pacinian and non-pacinian systems with hand-transmitted vibration detected from masked thresholds', *Somatosensory and Motor Research*, Vol. 22, Nos. 1–2, pp.69–84.

Morioka, M. and Griffin, M.J. (2006) 'Magnitude-dependence of equivalent comfort contours for fore-and-aft, lateral and vertical whole-body vibration', *Journal of Sound and Vibration*, Vol. 298, pp.755–772.

Morioka, M. and Griffin, M.J. (2010) 'Magnitude-dependence of equivalent comfort contours for fore-and-aft, lateral and vertical vibration at the foot for seated persons', *Journal of Sound and Vibration*, Vol. 329, pp.2939–2952.

Morioka, M. and Griffin, M.J. (2015) 'Masking of thresholds for the perception of fore-and-aft vibration of seat backrests', *Applied Ergonomics*, Vol. 50, pp.200–206.

Mulder, M. and Abbink, D.A. (2016) 'Subjective perception of discomfort due to vehicle vibrations in the sagittal plane', *IFAC-PapersOnLine*, Vol. 49, No. 19, pp.494–499.

Nawayseh, N. and Griffin, M.J. (2003) 'Non-linear dual-axis biodynamic response to vertical whole-body vibration', *Journal of Sound and Vibration*, Vol. 268, pp.503–523.

Nawayseh, N. and Griffin, M.J. (2004) 'Tri-axial forces at the seat and backrest during whole-body vertical vibration', *Journal of Sound and Vibration*, Vol. 277, pp.309–326.

Nawayseh, N. and Griffin, M.J. (2005a) 'Non-linear dual-axis biodynamic response to fore-and-aft whole-body vibration', *Journal of Sound and Vibration*, Vol. 282, pp.831–862.

Nawayseh, N. and Griffin, M.J. (2005b) 'Tri-axial forces at the seat and backrest during whole-body fore-and-aft vibration', *Journal of Sound and Vibration*, Vol. 281, pp.921–942.

Oxenham, A. (2001) 'Forward masking: Adaptation or integration?', *The Journal of the Acoustical Society of America*, Vol. 109, No. 2, pp.732–741.

Oxenham, A. and Plack, C. (2000) 'Effects of masker frequency and duration in forward masking: further evidence for the influence of peripheral nonlinearity', *Hearing Research*, Vol. 150, pp.258–266.

Penner, M., Cudahy, E. and Jenkins, G. (1974) 'The effect of masker duration on forward and backward masking', *Perception and Psychophysics*, Vol. 15, No. 3, pp.405–410.

Plack, C. and Oxenham, A. (1998) 'Basilar-membrane nonlinearity and the growth of forward masking', *The Journal of the Acoustical Society of America*, Vol. 103, No. 3, pp.1598–1608.

Qiu, Y. and Griffin, M.J. (2012) 'Biodynamic response of the seated human body to single-axis and dual-axis vibration: Effect of backrest and non-linearity', *Industrial Health*, Vol. 50, pp.37–51.

Rakheja, S. and Stiharu, I. (2002) 'Seated occupant apparent mass characteristics under automotive postures and vertical vibration', *Journal of Sound and Vibration*, Vol. 253, No. 1, pp.57–75.

Toward, M.G.R. and Griffin, M.J. (2011) 'The transmission of vertical vibration through seats: Influence of the characteristics of the human body', *Journal of Sound and Vibration*, Vol. 330, pp.6526–6543.

Wyllie, I.H. and Griffin, M.J. (2009) 'Discomfort from sinusoidal oscillation in the pitch and fore-and-aft axes at frequencies between 0.2 and 1.6 Hz', *Journal of Sound and Vibration*, Vol. 324, pp.453–467.

Zhou, Z. and Griffin, M.J. (2014) 'Response of the seated human body to whole-body vertical vibration: discomfort caused by sinusoidal vibration', *Ergonomics*, Vol. 57, No. 5, pp.714–732.

Zwicker, E. (1965a) 'Temporal effects in simultaneous masking and loudness', *The Journal of the Acoustical Society of America*, Vol. 38, pp.132–141.

Zwicker, E. (1965b) 'Temporal effects in simultaneous masking by white-noise bursts', *The Journal of the Acoustical Society of America*, Vol. 37, pp.653–663.

Zwicker, E. (1984) 'Dependence of post-masking on masker duration and its relation to temporal effects in loudness', *The Journal of the Acoustical Society of America*, Vol. 75, No. 1, pp.219–223.

Zwicker, E. and Zwicker, U.T. (1984) 'Binaural masking-level differences in non-simultaneous masking', *Hearing Research*, Vol. 13, pp.221–228.

Zwislocki, J., Pirodda, E. and Rubin, H. (1959) 'On some poststimulatory effects at the threshold of audibility', *The Journal of the Acoustical Society of America*, Vol. 31, No. 1, pp.9–14.

Appendix

A1 Results

Table A1 Rounded probability values of the Wilcoxon signed rank test

$\Delta t = 0$ s						
R_{MDoM}	*+tx*	*+ty*	*+tz*	*+rx*	*+ry*	*+rz*
0.5	0.0469	0.0005	0.0078	0.0005	0.0195	0.001
1	0.1094	0.0005	0.0005	0.0005	0.001	0.0005
2	0.4604	0.0005	0.0005	0.0005	0.0122	0.0005
4	0.4429	0.0005	0.0005	0.0005	0.0015	0.0005
$\Delta t = 0.58$ s						
0.5	0.1250	0.0078	0.0313	0.0078	0.0625	0.125
1	0.0234	0.001	0.1875	0.0039	0.0156	0.0313
2	0.0762	0.0005	0.0039	0.0005	0.001	0.001
4	1	0.0005	0.001	0.0005	0.0005	0.0005
$\Delta t = 1.08$ s						
0.5	0.0156	0.0039	0.125	0.0078	0.25	0.25
1	0.0156	0.001	0.25	0.0078	0.0313	0.0313
2	0.001	0.0005	0.0625	0.002	0.0039	0.0156
4	0.0264	0.0005	0.001	0.001	0.0005	0.0039
$\Delta t = 1.58$ s						
0.5	0.0313	0.0625	0.125	0.125	1	0.25
1	0.0625	0.0078	0.25	0.0156	0.125	0.125
2	0.0039	0.002	0.125	0.002	0.0039	0.125
4	0.001	0.0005	0.0156	0.001	0.002	0.0156
$\Delta t = 2.58$ s						
0.5	0.0625	0.125	0.125	0.25	0.5	0.125
1	1	0.125	1	1	1	1
2	0.1563	0.0156	0.25	0.0625	0.0625	0.5
4	0.002	0.001	0.125	0.0039	0.0156	0.5
$\Delta t = 4.58$ s						
0.5	0.5	0.25	0.5	0.5	1	1
1	0.75	0.5	1	1	1	1
2	0.125	0.0625	0.5	0.0625	0.25	0.25
4	0.125	0.0625	0.125	0.0313	0.125	0.5

A2 Discussion

Figure A1 Fitting curves and correlation values r for $G_{+tx}(R_{+tx}, \Delta t)$ with the distributions of $\underline{\boldsymbol{G}}_{+tx}(R_{+tx}, \Delta t)$

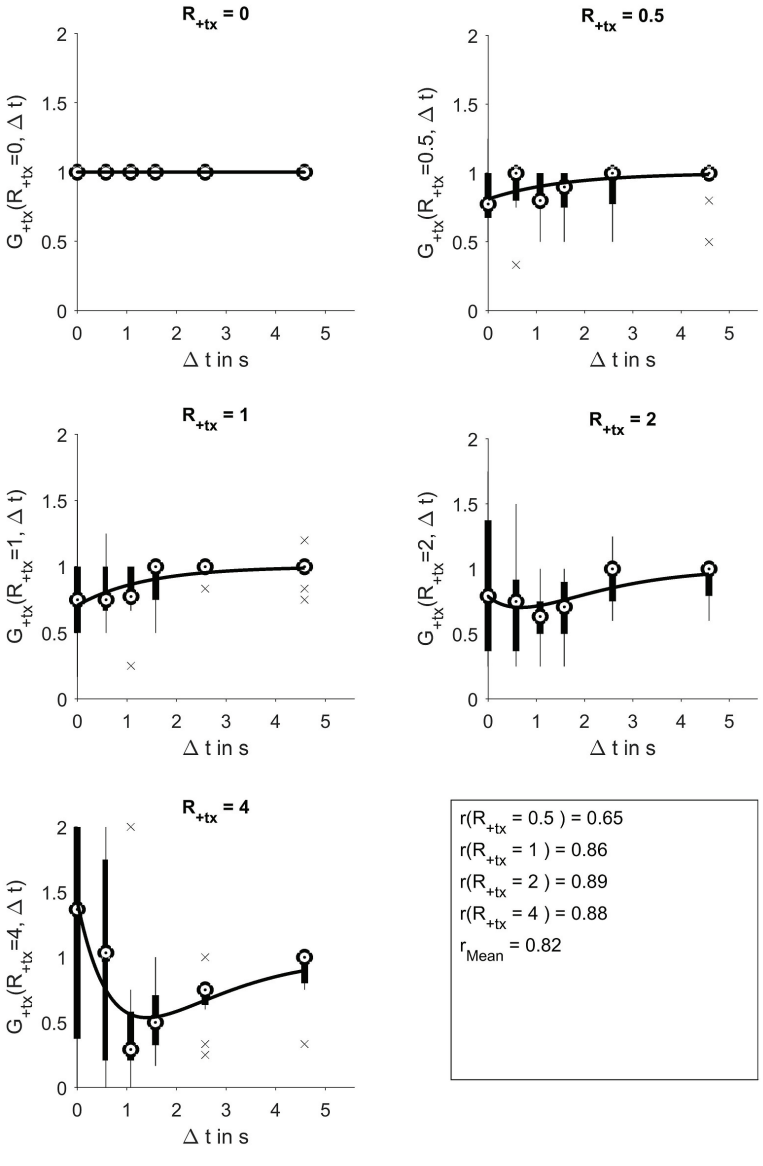

Figure A2 Fitting curves and correlation values r for $G_{+tz}(R_{+tz}, \Delta t)$ with the distributions of $\underline{\boldsymbol{G}}_{+tz}(R_{+tz}, \Delta t)$

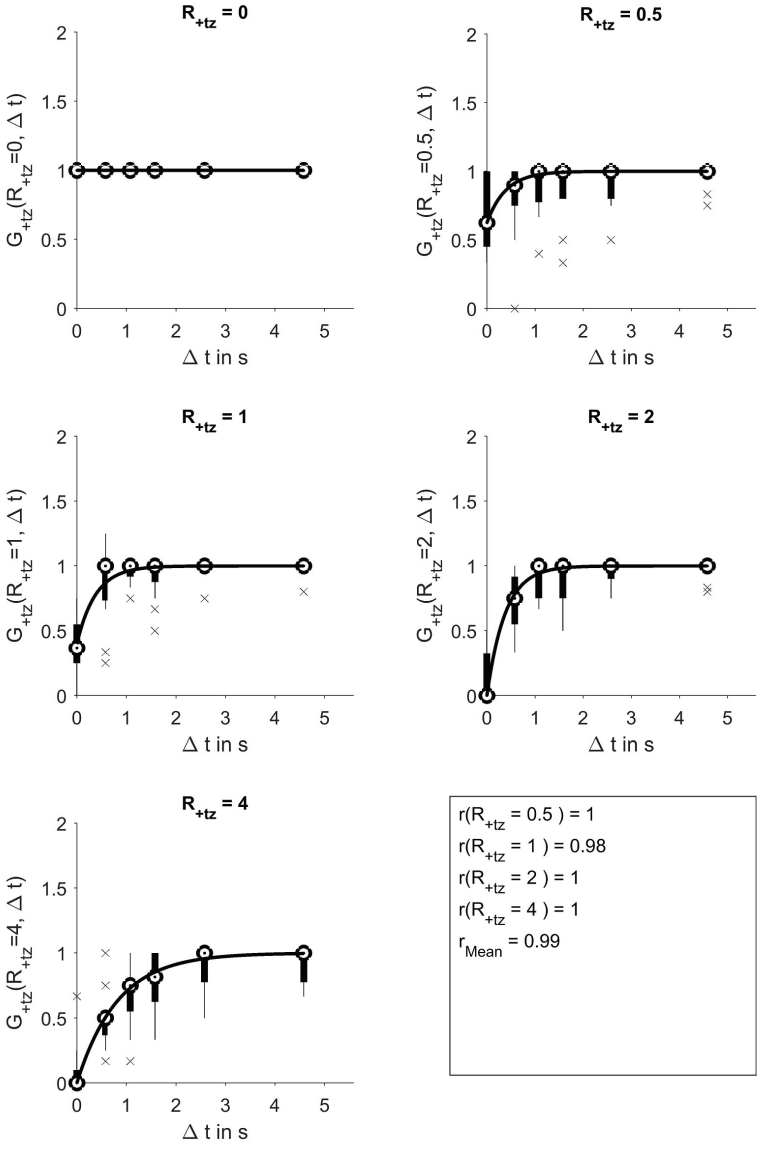

Figure A3 Fitting curves and correlation values r for $G_{+rx}(R_{+rx}, \Delta t)$ with the distributions of $\underline{\boldsymbol{G}}_{+rx}(R_{+rx}, \Delta t)$

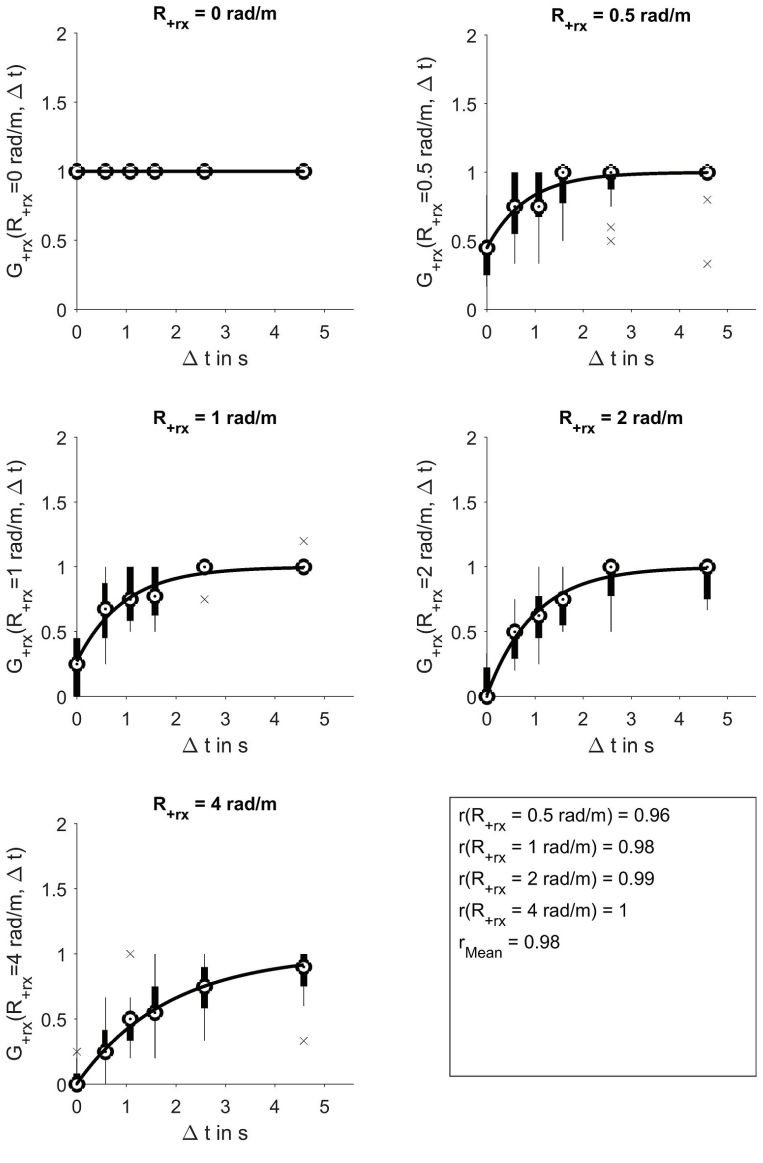

Figure A4 Fitting curves and correlation values r for $G_{+ry}(R_{+ry}, \Delta t)$ with the distributions of $\underline{\boldsymbol{G}}_{+ry}(R_{+ry}, \Delta t)$

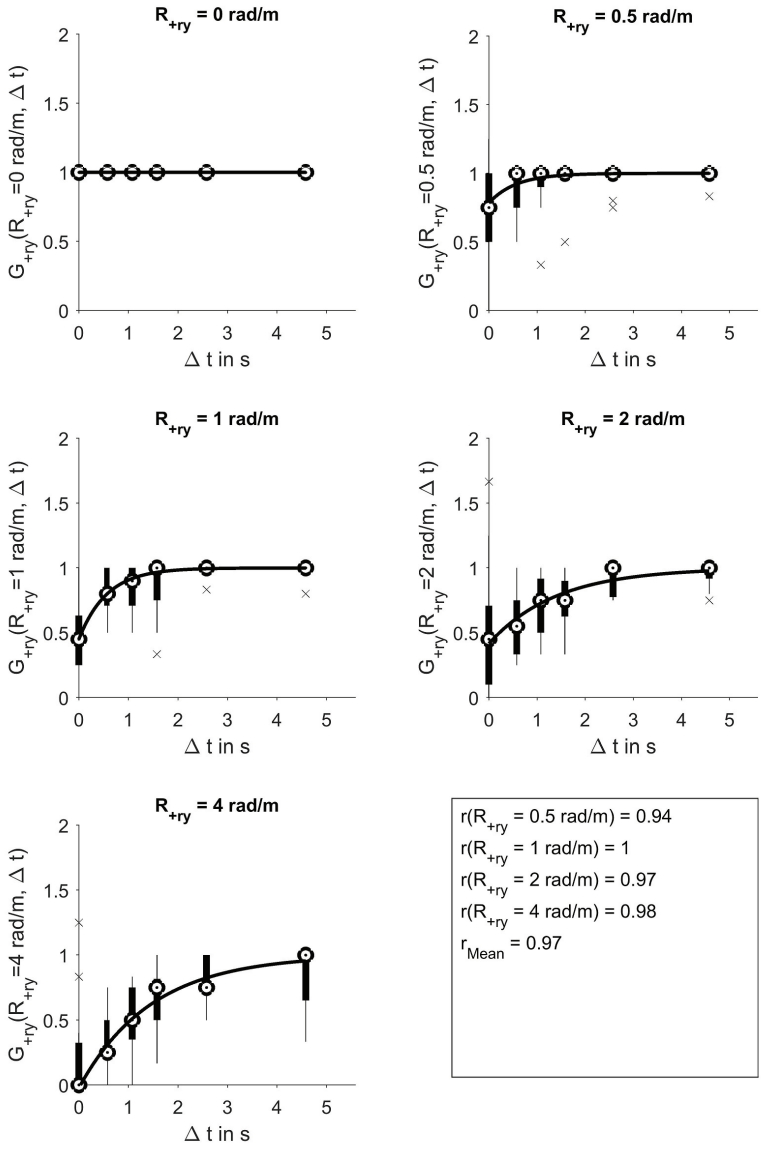

Figure A5 Fitting curves and correlation values r for $G_{+rz}(R_{+rz}, \Delta t)$ with the distributions of $\underline{\boldsymbol{G}}_{+rz}(R_{+rz}, \Delta t)$